Quantitative imaging of sheet resistance with a scanning near-field microwave microscope

D. E. Steinhauer,[a] C. P. Vlahacos, S. K. Dutta, B. J. Feenstra, F. C. Wellstood, and Steven M. Anlage
Department of Physics, Center for Superconductivity Research, University of Maryland, College Park, Maryland 20742-4111

(Received 7 October 1997; accepted for publication 11 December 1997)

We describe quantitative imaging of the sheet resistance of metallic thin films by monitoring frequency shift and quality factor in a resonant scanning near-field microwave microscope. This technique allows fast acquisition of images at approximately 10 ms per pixel over a frequency range from 0.1 to 50 GHz. In its current configuration, the system can resolve changes in sheet resistance as small as 0.6 $\Omega/\square$ for 100 $\Omega/\square$ films. We demonstrate its use at 7.5 GHz by generating a quantitative sheet resistance image of a $YBa_2Cu_3O_{7-\delta}$ thin film on a 5 cm diam sapphire wafer. © *1998 American Institute of Physics.* [S0003-6951(98)00307-6]

Nondestructive imaging of microwave sheet resistance has been demonstrated using a variety of probes combined with resonant systems. Far-field techniques, such as confocal[1,2] and dielectric[3,4] resonators, while allowing quantitative sheet resistance imaging, have the disadvantage of relatively low spatial resolution ($\gtrsim 1$ mm) limited by the wavelength. Near-field microscopy using coaxial,[5,6] microstrip,[7] or waveguide[8] resonators, offers higher spatial resolution. However, current techniques either require contact with the sample,[6] inhibiting quantitative interpretation of the data, have low sheet resistance sensitivity in conducting samples,[5,7,9] or require additional image processing to obtain sub-wavelength resolution.[8] For nondestructive sheet resistance imaging of thin films, it is desirable to have quantitative methods that combine high resolution, high speed, simple construction from commercially available components, and straightforward image interpretation. We describe here the application of an open-ended coaxial probe resonator to obtain quantitative images of microwave sheet resistance with $\lambda/80$ spatial resolution.

Our scanning microwave microscope consists of a resonant coaxial transmission line connected to an open-ended coaxial probe and a microwave source (Fig. 1).[10–12] The microwave source, which is weakly coupled to the resonant transmission line through a decoupling capacitor C_D, is frequency modulated by an external oscillator at a rate $f_{FM} \sim 3$ kHz. The electric field at the probe tip is perturbed by the region of the sample beneath the probe's center conductor. We monitor these perturbations using a diode detector which produces a voltage signal proportional to the power reflected from the resonator. A feedback circuit[12] (Fig. 1) keeps the microwave source locked to a resonant frequency of the transmission line, and has a voltage output which is proportional to shifts in the resonant frequency due to the sample.

To determine the quality factor Q of the resonant circuit, a lock-in amplifier, referenced at $2f_{FM}$, gives an output voltage $V_{2f_{FM}}$ which is related to the curvature of the reflected power versus frequency curve on resonance, and hence to Q. To relate $V_{2f_{FM}}$ and Q, we perform a separate experiment, in which we vary Q using a microwave absorber at various heights below the probe tip, and measure the absolute reflection coefficient $|\rho|^2$ of the resonator. If $|\rho_0|^2$ is the reflection coefficient at a resonant frequency f_0, then the coupling coefficient between the source and the resonator is $\beta = (1 - |\rho_0|)/(1 + |\rho_0|)$. The loaded quality factor of the resonator[13,14] is $Q_L = f_0/\Delta f$, where Δf is the difference in frequency between the two points where $|\rho|^2 = (1+\beta^2)/(1+\beta)^2$. The unloaded quality factor, which is the Q of the resonator without coupling to the microwave source and detector, is then $Q_0 = Q_L(1+\beta)$. We also measure $V_{2f_{FM}}$, and

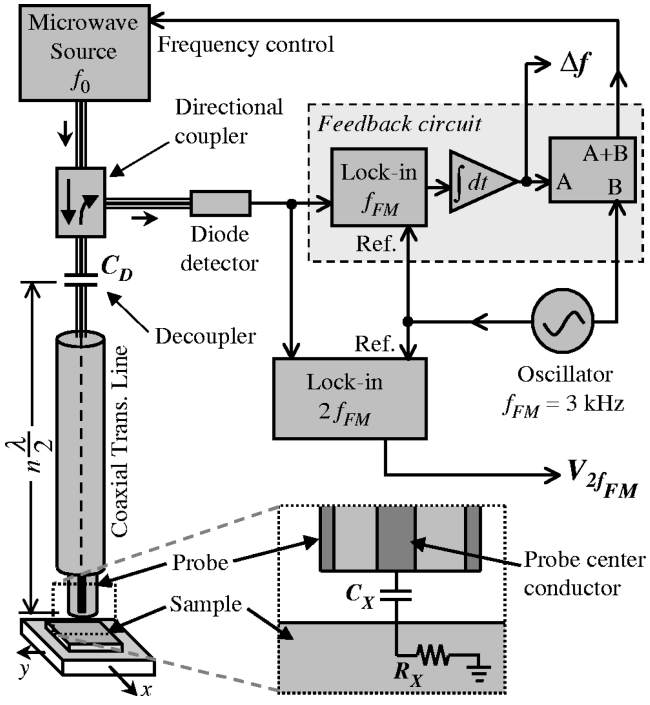

FIG. 1. Schematic of the scanning near-field microwave microscope. The inset shows the interaction between the probe and the sample, represented by a capacitance C_X and a resistance R_X.

[a]Color versions of the figures in this paper can be found at http://www.csr.umd.edu/research/hifreq/micr_microscopy.html; electronic mail: steinhau@squid.umd.edu

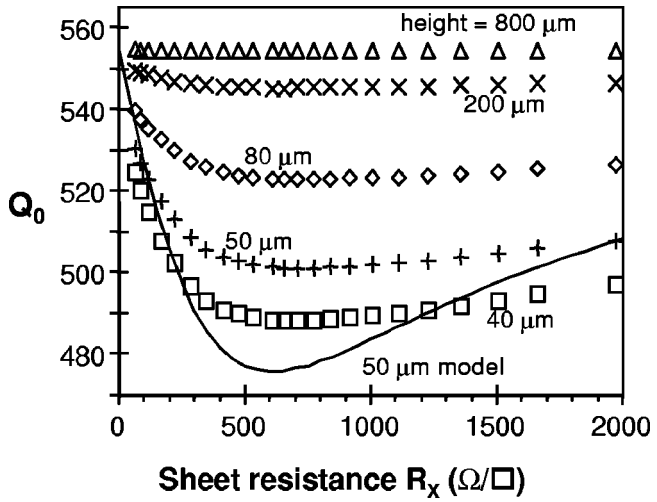

FIG. 2. Unloaded quality factor Q_0 of the resonant circuit as a function of the sheet resistance R_X of a variable-thickness aluminum thin-film sample. The labels indicate different probe-sample separations. A probe with a 500 μm center conductor was used at a frequency of 7.5 GHz. The solid line indicates a model calculation for a probe-sample separation of 50 μm.

find that there is a unique functional relationship between Q_0 and $V_{2f_{FM}}$; thus, we need to calibrate this relationship only once for a given microscope resonance. In a typical scan, we record $V_{2f_{FM}}$, and afterward convert $V_{2f_{FM}}$ to Q_0.

To determine the relationship between Q_0 and sample sheet resistance (R_X), we used a variable-thickness aluminum thin film on a glass substrate.[12] The cross section of the thin film is wedge shaped, implying a spatially varying sheet resistance. Using a probe with a 500 μm diam center conductor, and selecting a resonance of the microscope with a frequency of 7.5 GHz, we acquired frequency shift and Q_0 data. We then cut the sample into narrow strips to take two-point resistance measurements and determine the local sheet resistance. The unloaded Q_0 of the resonator as a function of R_X is shown in Fig. 2 for various probe-sample separations. We note that Q_0 reaches a maximum as $R_X \to 0$; as R_X increases, Q_0 drops due to loss from currents induced in the sample, reaching a minimum around $R_X = 660\ \Omega/\square$ for a height of 50 μm. Similarly, as $R_X \to \infty$, Q_0 increases due to diminishing currents in the sample.

We also note that when the probe is located 50 μm above the bare glass substrate, $Q_0 = 549$, which is only slightly less than $Q' = 555$ when the probe is far away (>1 mm) from the sample. Using $1/Q_0 = 1/Q_s + 1/Q'$, we find $Q_s = 51000 \gg Q' = 555$, where Q_s is associated with losses in the glass substrate, and Q' is associated with losses in the transmission line. As a result, we conclude that the glass substrate has little effect on Q_0. In contrast, because the dielectric substrate effectively lengthens the microscope resonant circuit, frequency shift is highly sensitive to the substrate.[12,15] This suggests that we use the Q data, rather than the frequency shift data, to generate substrate-independent images of thin film sheet resistance.

As shown in Fig. 2, R_X is a double-valued function of Q_0. This presents a problem for converting the measured Q_0 to R_X. However, R_X is a single-valued function of the frequency shift,[12] allowing one to use the frequency shift data to determine which branch of the $R_X(Q)$ curve should be used.

To better understand the system's behavior, we modeled the interaction between the probe and sample as a capacitance C_X between the probe's center conductor and the sample in series with the sample sheet resistance R_X (see Fig. 1).[12,15] We assumed a parallel plate approximation for the capacitor C_X, and took $R_X = \tilde{\rho}/t$,[12] where $\tilde{\rho}$ is the sample dc resistivity, and t is the film thickness. To find Q_0, we calculated the width of the resonant minimum in the reflection coefficient $|\rho|^2$ versus frequency curve, as described above. The model results for a height of 50 μm are indicated by the solid line in Fig. 2. To fit the data we used the measured $Q_0 = 555$ and $Q_L = 353$ with the probe far away from the sample to fix two fitting parameters: the coupling capacitance $C_D = 0.17$ pF, and the transmission line attenuation constant $\alpha = -1.26$ dB/m (in close agreement with the manufacturer's specified value[16] of $\alpha = -1.23$ dB/m). Aside from a coupling factor involving C_X, the model agrees qualitatively and predicts the R_X which yields the minimum Q_0 to within 10%. For large R_X, the model predicts a faster return to the asymptotic Q_0 value of 555. The overall behavior of this simple model confirms our understanding of the system.

To explore the capabilities of our system, we scanned a thin film of $YBa_2Cu_3O_{7-\delta}$ (YBCO) on a 5 cm diam sapphire substrate at room temperature. The film was deposited using pulsed laser deposition with the sample temperature controlled by radiant heating. The sample was rotated about its center during deposition, with the ~ 3 cm diam plume held at a position halfway between the center and the edge. The thickness of the YBCO thin film varied from about 100 nm at the edge to 200 nm near the center.

Figure 3 shows three microwave images of the YBCO sample. The frequency shift [Fig. 3(a)] and Q_0 [Fig. 3(b)] were acquired simultaneously, using a probe with a 500 μm diam center conductor at a height of 50 μm above the sample. The scan took approximately 10 min to complete, with raster lines 0.5 mm apart. The frequency shifts in Fig. 3(a) are relative to the resonant frequency of 7.5 GHz when the probe was far away (>1 mm) from the sample; the resonant frequency shifted downward by more than 2.2 MHz when the probe was above the center of the sample. Noting that the resonant frequency drops monotonically between the edge and the center of the film, and that the resonant frequency is a monotonically increasing function of sheet resistance,[12] we conclude that the sheet resistance decreases monotonically between the edge and the center.

The frequency shift and Q_0 images [Figs. 3(a) and 3(b)] differ slightly in the shape of the contour lines. This is most likely due to the 300 μm thick substrate being warped, causing a variation of a few microns in the probe-sample separation during the scan. However, for a sample such as that shown in Fig. 3, with an R_X variation across the sample of $\sim 100\ \Omega/\square$, the Q_0 data are primarily sensitive to changes in R_X, while the frequency shift data are primarily sensitive to changes in probe-sample separation. As a result, we attribute the difference between the frequency shift and Q_0 images to small changes in probe-sample separation, which will mainly affect the frequency shift data. Since the values of R_X are

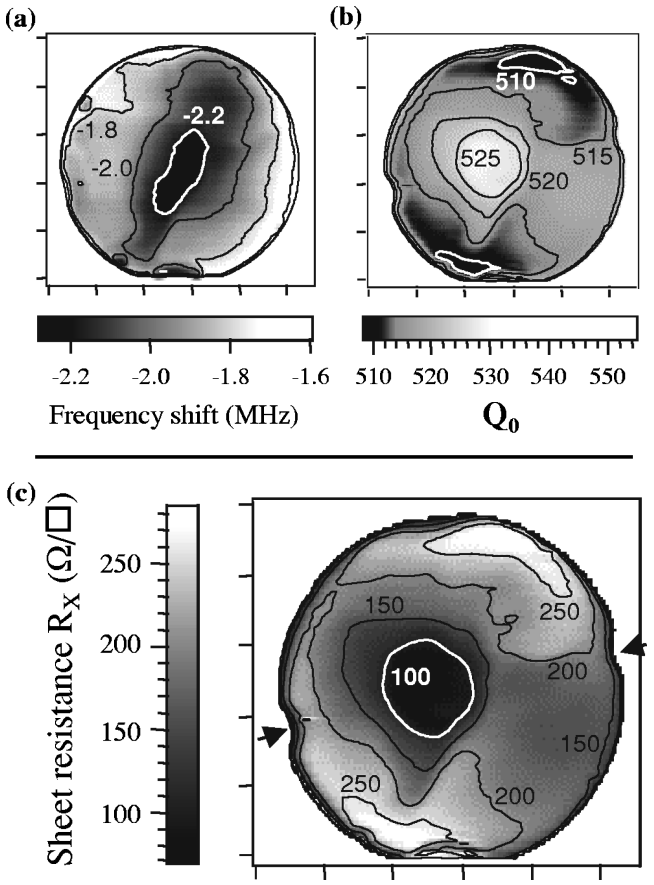

FIG. 3. Images of a variable-thickness YBCO thin-film on a 5 cm diam sapphire wafer, where the film is the thickest at the center. The tick marks are 1 cm apart for the images of (a) frequency shift relative to the resonant frequency when the probe is far away (>1 mm) from the sample, (b) unloaded Q, and (c) sheet resistance (R_X). The arrows in (c) point to small semi-circular regions where clips held the wafer during deposition, and thus no film is present. The labels indicate values at each contour line. A probe with a 500 μm diam center conductor was used at a height of 50 μm, at a frequency of 7.5 GHz.

retrieved from the Q data, the warping does not affect the final R_X appreciably. In principle, one can use the combined frequency shift and Q images to extract sample topography information,[15] allowing one to separate the effects of sample sheet resistance and topography.

From Fig. 3(b), we see that the lowest Q occurs near the edge of the film, and that the Q rises toward the center of the sample. As mentioned above, R_X is not a single-valued function of Q and we must use the frequency shift image [Fig. 3(a)] to determine which branch of the Q_0 versus R_X curve in Fig. 2 to use. From the frequency shift image we learned that R_X decreases monotonically from the edge to the center of the sample; therefore we use the branch of the Q_0 versus R_X curve with $R_X<660$ Ω/□, since this is the branch that yields a decreasing R_X for increasing Q_0.

With the appropriate branch identified, we then transformed the Q image in Fig. 3(b) to the sheet resistance image in Fig. 3(c) using a polynomial least-squares fit to the data presented in Fig. 2 for $R_X<540$ Ω/□ and a height of 50 μm. Figure 3(c) confirms that the film does indeed have a lower resistance near the center, as was intended when the film was deposited. We note that the sheet resistance does not have a simple radial dependence, due to either nonstoichiometry or defects in the film.

After scanning the YBCO film, we patterned it and made four-point dc resistance measurements all over the wafer. The dc sheet resistance had a spatial dependence identical to the microwave data in Fig. 3(c). However, the absolute values were approximately twice as large as the microwave results, most likely due to degradation of the film during patterning.

To estimate the sheet resistance sensitivity, we monitored the noise in $V_{2f_{FM}}$. We find the Q sensitivity of the system to be $\Delta Q_0 \approx 0.08$ for $Q_0=555$ and an averaging time of 10 ms. Combining this with the data in Fig. 2, we find $\Delta R_X/R_X=6.4\times10^{-3}$, for $R_X=100$ Ω/□ using a probe with a 500 μm diam center conductor at a height of 50 μm and a frequency of 7.5 GHz. The sensitivity scales with the capacitance between the probe center conductor and the sample (C_X); increasing the diameter of the probe center conductor and/or decreasing the probe-sample separation would improve the sensitivity.

In conclusion, we have demonstrated a technique which uses a near-field microwave microscope to generate quantitative sheet resistance images of thin film samples. The strengths of our system include the ability to arrive at quantitative results and to confirm our understanding of the system with a simple model. Other advantages include its speed, measurement frequency bandwidth, construction from standard commercially available components, and the possibility of enhancing its spatial resolution by using a probe with a smaller diameter center conductor.[10]

The authors would like to thank Alberto Pique of Neocera, Inc., for the YBCO wafers. This work has been supported by NSF-MRSEC Grant No. DMR-9632521, NSF Grant Nos. ECS-9632811 and DMR-9624021, and by the Center for Superconductivity Research.

[1] S. Hogan, S. Wagner, and F. S. Barnes, Appl. Phys. Lett. **35**, 77 (1979).
[2] J. S. Martens, V. M. Hietala, D. S. Ginley, T. E. Zipperian, and G. K. G. Hohenwarter, Appl. Phys. Lett. **58**, 2543 (1991).
[3] J. Gallop, L. Hao, and F. Abbas, Physica C **282–287**, 1579 (1997).
[4] C. Wilker, Z-Y. Shen, V. X. Nguyen, and M. S. Brenner, IEEE Trans. Appl. Supercond. **3**, 1457 (1993).
[5] C. A. Bryant and J. B. Gunn, Rev. Sci. Instrum. **36**, 1614 (1965).
[6] I. Takeuchi, T. Wei, F. Duewer, Y. K. Yoo, X.-D. Xiang, V. Talyansky, S. P. Pai, G. J. Chen, and T. Venkatesan, Appl. Phys. Lett. **71**, 2026 (1997).
[7] M. Tabib-Azar, N. S. Shoemaker, and S. Harris, Meas. Sci. Technol. **4**, 583 (1993).
[8] M. Golosovsky, A. Galkin, and D. Davidov, IEEE Trans. Microwave Theory Tech. **44**, 1390 (1996).
[9] Y. Xu and R. G. Bosisio, IEE Proc.-H **139**, 500 (1992).
[10] C. P. Vlahacos, R. C. Black, S. M. Anlage, A. Amar, and F. C. Wellstood, Appl. Phys. Lett. **69**, 3274 (1996).
[11] S. M. Anlage, C. P. Vlahacos, S. Dutta, and F. C. Wellstood, IEEE Trans. Appl. Supercond. **7**, 3686 (1997).
[12] D. E. Steinhauer, C. P. Vlahacos, S. K. Dutta, F. C. Wellstood, and S. M. Anlage, Appl. Phys. Lett. **71**, 1736 (1997).
[13] J. E. Aitken, Proc. IEE **123**, 855 (1976).
[14] K. Zaki and G. J. Chen (private communication).
[15] C. P. Vlahacos, D. E. Steinhauer, S. K. Dutta, B. J. Feenstra, S. M. Anlage, and F. C. Wellstood (unpublished).
[16] W. L. Gore and Assoc., Inc. (private communication). (See also Ref. 12 of Ref. 12).